Seminaria UZ3 2023
Zakład Energetyki Jądrowej i Badań Środowiskowych
UZ3

Preliminary Experimental Comparison of Fast Neutron Measurement by Np237 Fission to Capture Ratio and Reverse Dark Current of Planar Silicon Detector Methods.

Marcin Szuta,
National Cenntre for Nuclear Research, Otwock-Swierk 05-400, Poland
E-mail: marcin.szuta@ncbj.gov.pl

NCBJ
ŚWIERK

Impact of Average Neutron Energy on the Fast Neutron Fluency Measurement by Np237 Fission to Capture Ratio and Reverse Dark Current of Planar Silicon Detector Methods.

Outline

1. Introduction

- It is a subsequent step of feasibility study of fast neutron fluency measurement using two different complementary methods [1].
- We have focused on the efficiency dependence of incineration the minor actinides on the distance of their samples from the neutron spallation source.
- So far, we have not been able to place actinide samples in any place other than the lead specimen window.

1. Introduction

- We have processed the experimental data of irradiated Np- 237 actinide samples and silicon detectors directly placed on sections 2 and 4 of the QUINTA setup (see Fig. 1) without lead shield-reflector.
- These samples were 12 cm from the source of the neutron spallation source, what is about 8 cm closer than before when we placed the actinides samples in the window of the lead shield-reflector.

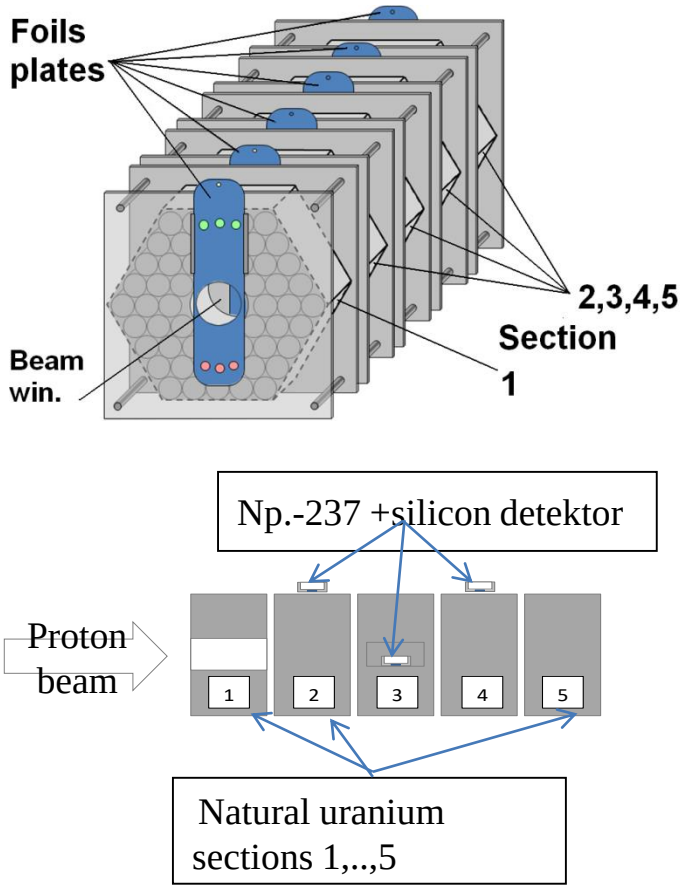

Fig. 1 Target of QUINTA assembly.

M. Szuta
National Centre for Nuclear Research, Poland

1. Introduction

- The idea of the first method is to search the neutron energy for the ratio of fission cross section to capture cross section of the selected actinide isotope from the nuclear data base that is equal to the measured ratio of fissioned and captured actinide isotope Np-237.
- The idea of the second method is measurement of fast neutron irradiation induced reverse dark current increase of planar silicon detectors which is linearly proportional to neutron fluence.

2. Fast neutron fluence measurement methods
2.1a. Actinide fast neutron fluence measurement method.

- The fast neutron fluence measurement method consists in utilizing neutron irradiated actinide samples for estimating neutron fluence and average neutron energy inside the volume of samples. The idea is to search the neutron energy (E_d) for the ratio ($\alpha(E_d)$) of fission cross section ($\sigma_f(E_d)$) to capture cross section ($\sigma_c(E_d)$) of the selected actinide isotope from the nuclear data base that is equal to the measured ratio (α_m) of fissioned (N_{yf}) and captured (N_{yc}) actinide isotopes (spectral indexes):

$$\alpha(E_d) = \frac{\sigma_f(E_d)}{\sigma_c(E_d)} = \alpha_m = \frac{N_{yf}}{N_{yc}} = \frac{\overline{\sigma}_f}{\overline{\sigma}_c}$$

2. Fast neutron fluence measurement methods

2.1a. Actinide fast neutron fluence measurement method.

Since the measured spectral indexes (α_m) is defined as the ratio of average fission ($\bar{\sigma}_f$) and capture ($\bar{\sigma}_c$) cross sections so the ratio ($\alpha(E_d)$ of retrieved distinct fission ($\sigma_f(E_d)$) and capture ($\sigma_c(E_d)$) cross sections for the distinct neutron energy (E_d) from the nuclear data base describe the average values:

$E_d = \bar{E}$; $\sigma_f(E_d) = \bar{\sigma}_f$; $\sigma_c(E_d) = \bar{\sigma}_c$

Having the average fission and capture cross section values we can evaluate the average neutron flux ($\bar{\phi}$) in the location of the actinide sample using the measured amount of fissioned and captured actinide isotopes.

2. Fast neutron fluence measurement methods
2.1a. Actinide fast neutron fluence measurement method.

- The amount of neutron induced fissioned (N_{yf}) and neutron captured actinide isotopes (N_{yc}) in the actinide sample of volume V_p can be expressed:
- $$N_{yf} = V_p \, \bar{\phi} \, N \, \bar{\sigma}_f \, t \qquad (1)$$
- $$N_{yc} = V_p \, \bar{\phi} \, N \, \bar{\sigma}_c \, t \qquad (2)$$

Where

V_p - actinide sample volume [cm^3],

$\bar{\Phi}$ - average neutron flux in the place of actinide sample location [$n/cm^2 \cdot s$],

N – number of actinide isotopes in volume unit [cm^{-3}],

$\bar{\sigma}_f$; $\bar{\sigma}_c$ -average microscopic cross section for the reactions (n, f) and (n, γ) respectively [barns],

t - irradiation time [s].

2. Fast neutron fluence measurement methods
2.1a. Actinide fast neutron fluence measurement method.

- Two different equations for fissioned (N_{yf}) and captured (N_{yc}) actinide isotopes should give the same average neutron flux value what is a proof for correct measurements.

$$\frac{N_{yf}}{N_{yc}} = \frac{V_p \, \bar{\phi} \, N \, \bar{\sigma}_f \, t}{V_p \, \bar{\phi} \, N \, \bar{\sigma}_c \, t} = \frac{\bar{\sigma}_f}{\bar{\sigma}_c}$$

2. Fast neutron fluence measurement methods
2.1a. Actinide fast neutron fluence measurement method

- It is useful to look closely at the ratios $\alpha = \sigma_f / \sigma_c$ of the capture and fission cross section of the Np.-237 isotope.
- The fission/absorption ratios are consistently higher for the fast-neutron spectrum. Thus, in a fast spectrum, actinides are preferentially fissioned, not transmuted into higher actinides.

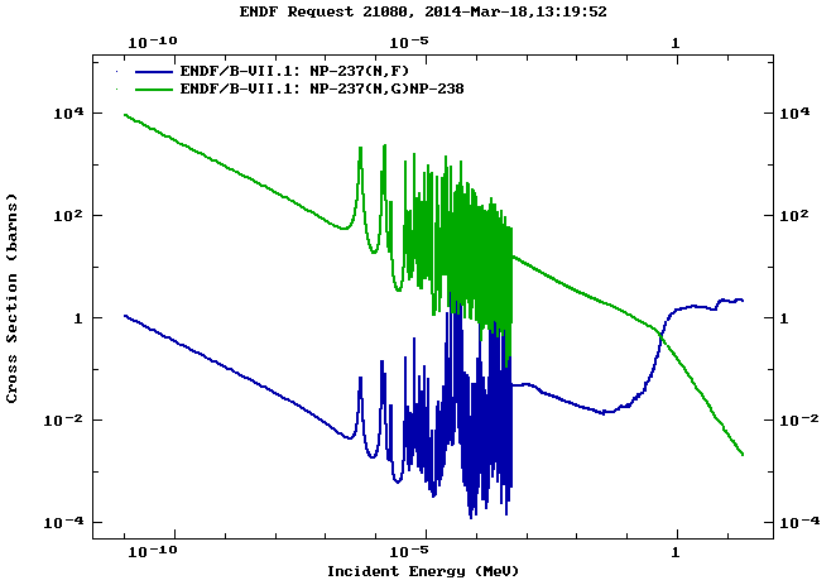

Fig. 1a. Cross-sections of Np-237(n,g)Np-238 and Np-237(n,f) reactions.

2. Fast neutron fluence measurement methods
2.1b. Silicon semiconductor fast neutron fluence measurement method.

- Fast neutrons with energy of E_n>100 keV produces damage in the volume of silicon semiconductor in the form of vacancies in the crystal lattice (knocking-out primary atom from the lattice site).
- Reverse dark current of the detector grows linearly [2, 3] with increasing fast neutron fluence
- $\Delta I = \alpha_I \times V \times \Phi$, (3)
- where:
- $\Delta I = (I_{irrad.} - I_{nonirrad.})$, [A], increment detector current,
- **V**-volume of the detector, [cm^{-3}],
- **Φ**-neutron fluence, [cm^{-2}],
- α_I=(5±10%)×10^{-17} [A×cm^{-1}], constant of radiation damages.

2. Fast neutron fluence measurement methods
2.1b. Silicon semiconductor fast neutron fluence measurement method.

- Si detector under neutron irradiation changes its electrical parameters (characteristics) due to generation of radiation defects in the crystal lattice.
- The radiation defects leads among others to reverse current growth.
- In Fig.1b is presented the measured dependence of the reverse (dark) current on the fast neutron fluence for two planar detectors. The difference in slopes of these dependences is attributed to thickness variation (detector no. 1 was 10% thinner than detector no. 2) [2].

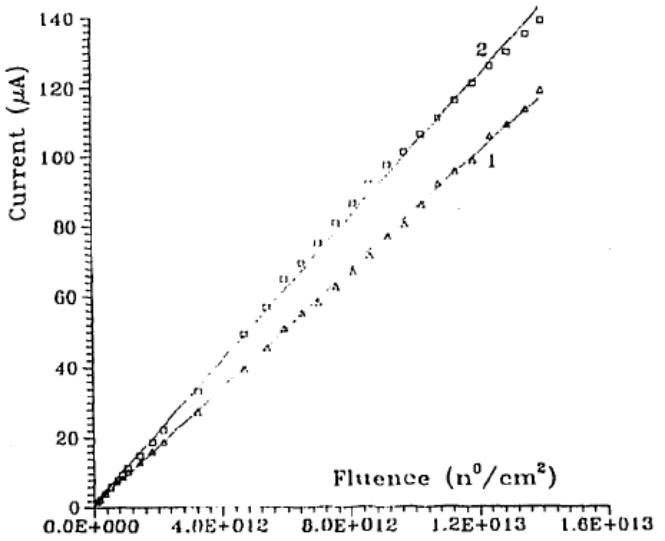

Fig.1b. Dependence of the reverse dark current at a temperature of +18°C on the fast neutron fluence for two detectors installed at one and the same site in neutron channel no. 11 of the IBR-2 reactor (JINR). These measurements were performed in 1991 [2].

2. Fast neutron fluence measurement methods
2.1b. Silicon semiconductor fast neutron fluence measurement method.

- Neutron radiation induced damage of silicon detectors presented in Fig. 1c is described by help of the parameter D(E) which is expressed in MeV x mb. It is understood that this is the product of neutron energy (in MeV) and the damage cross-section (in mb) of the crystal lattice of silicon detector.
- As it is seen the damage parameter D(E) in function of neutron energy starts to appear with threshold mode for the energy 100 keV.

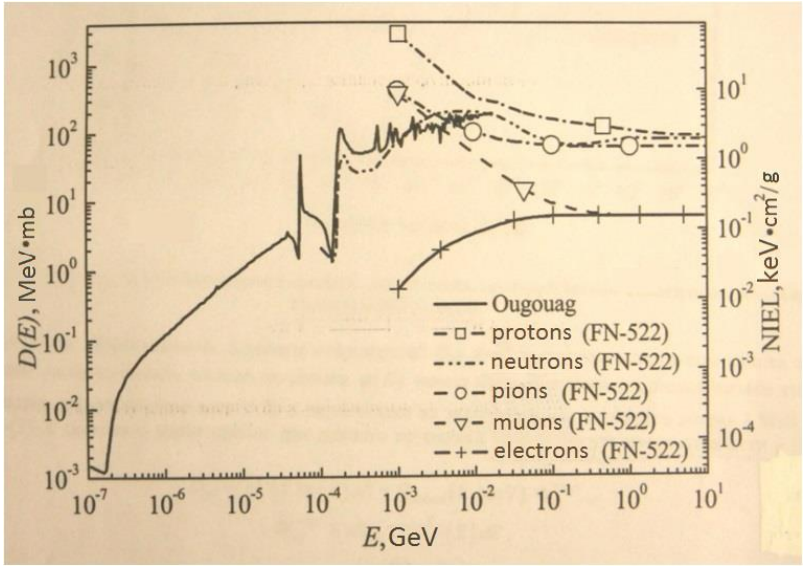

Fig. 1c. Function of defect formation of D(E) in MeV×mb, (Ougouag) and the function NIEL-FN-522 in keV×cm^2/g, (van Ginneken), [4].

2. Fast neutron fluence measurement methods
2.1b. Silicon semiconductor fast neutron fluence measurement method

- Mathematical construct of the equations describing the neutron fluence of the two methods are very alike (see equations 1, 2, and 3). In both methods the values which are proportional to the neutron fluence depends on cross section of neutron inducing damage in the silicon detector and cross sections of neutron inducing fission and capture on Np-237 minor actinide (see Fig. 2). The cross sections used in both methods depending on neutron energy are the primary reasons of final result (**ΔI and N_{yf} or N_{yc}**) which let us to evaluate the searched neutron fluence. The further similarity is that the volume of detectors of both methods are taken into account (consideration).

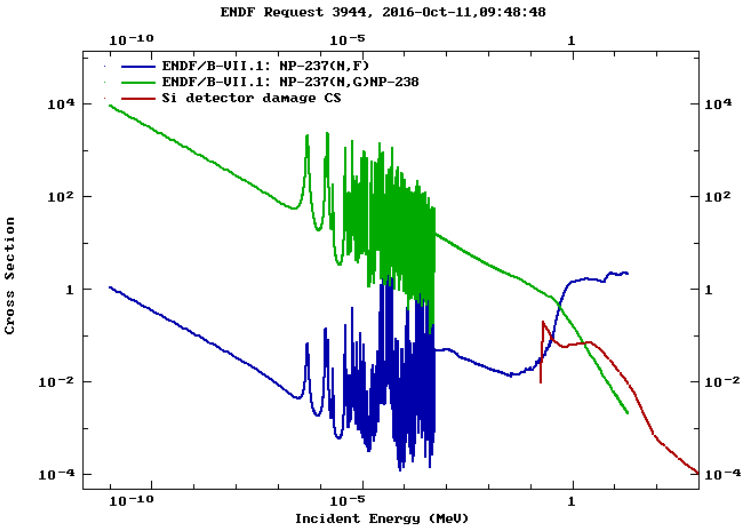

Fig. 2. Cross section of neutron inducing damage in the silicon detector (red curve [4]) and cross sections of neutron inducing fission and capture on Np-237 minor actinide.

2. Fast neutron fluence measurement methods
2.1b. Silicon semiconductor fast neutron fluence measurement method

- Neutron radiation induced damage of silicon detectors is presented in Fig. 2. The values of neutron damage cross section of silicon detectors in function of neutron energy presented in Fig.2, are extracted from the figure describing “Function of defect formation of D(E) in MeV×mb, (Ougouag) and the function NIEL-FN-522 in keV×cm^2/g,” presented in reference [4].
- The damage cross section in function of energy starts with the threshold mode for the energy about170 keV [4].

3. Measurement .

3.1. Irradiation details

- The Quinta target was irradiated with a pulsed proton beam of 0.66 GeV energy extracted from the Synchrotron accelerator, also located at the JINR. Total number of protons of the irradiation is equal to **$7.78\ 10^{14}$** during the time of irradiation equal to **11890 seconds (5h 15 min)**, (see Table 1). Prior to the irradiation, several polaroid films were placed on the front of Quinta to ensure the proton beam was striking in the centre of the beam window.

Table 1
Details of the two Quinta irradiations performed at the Synchrotron accelerator. Xc and Yc refer to the coordinates of the beam centre on the x–y plane.

Experimental session in May 2017	
Incident ion	Proton
Ion energy	0.66 GeV
Irradiation duration	5h 15 min
Protons on target	**$7.78\ 10^{14}$**
X_c (cm)	0.45 ± 0.02
Y_c (cm)	0.06 ± 0.02
$FWHM_x$ (cm)	2.73 ±0.3
$FWHM_y$ (cm)	3.22± 0.3

3. Measurement .
3.2 Results

- Gamma-ray spectrum analysis was carried out in a well established manner.
- The measured activities of considered isotopes at end of irradiation (EOI) were corrected for decay during the irradiation according to known deuteron beam profile, for decay between EOI and start of counting (cooling time) and for decay during the counting time and also not forgetting about dead time correction (t_{real}/t_{live}).
- Thus one can calculate the relative number of considered produced isotopes at the end of irradiation for each measurement.

3. Measurement .
3.2 Results

- From gamma-ray spectrum of the irradiated Np-237 we have selected the following fission products ^{133}I, ^{135}I, ^{97}Zr, ^{132}I and ^{92}Sr (see Table 2) which we have used to evaluate the fission rate per one gram Np-237 and per one deuteron applying the proper equations. For the I-135 two different gamma picks were used: 1131.51 keV and 1260.41.

- Table 2. Fission fragment data of fast neutron induced fission of Np.-237

Isotope	*$T_{1/2}$*	*γ line [keV]*	*I_γ [%]*	*γ_f [%] cumulate*
Sr-92	2.66h	1383.93	90	4.01
Zr-97	16.744h	507.64	5.03	5.35
I-132	2.295h	772.6	75.6	4.39
I-133	20.87h	529.87	87	4.45
I-135	6.57h	1260.41 1131.51	28.7 22.6	4.16

3. Measurement .
3.2 Results -cont.

Fig. 3

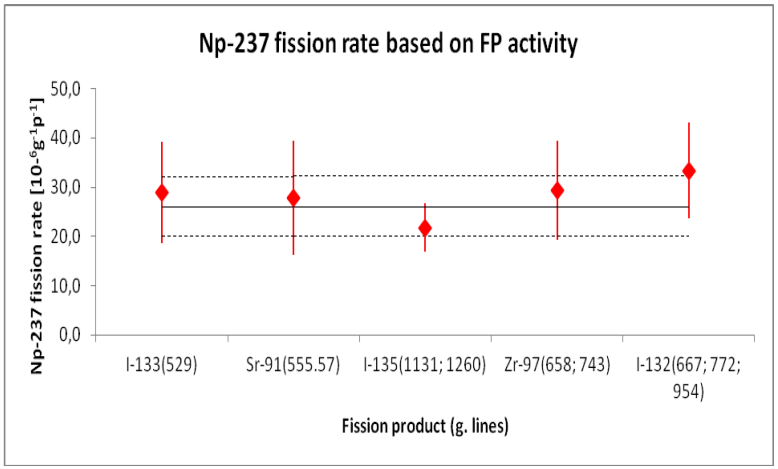

Fig. 3a

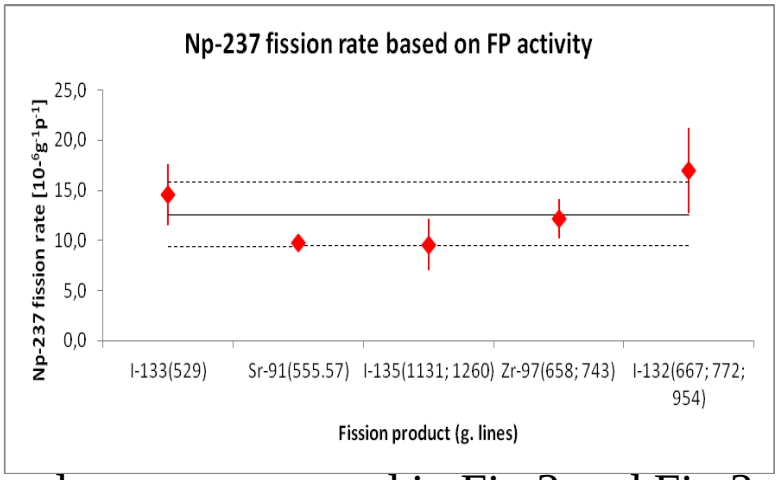

- The resulting normalized fission rate $I_{f\gamma}$ values are presented in Fig.3 and Fig.3a for deuteron beam of 0.66 GeV for the samples located on section 2 and 4 of the QUINTA target respectively.:
- Fig. 3. Fission rate for differet fission products of Np.-237 sample of 0.987 g weight for proton beam of 0.66 GeV energy located on section 2 of the QUINTA target.
- Fig. 3a. Fission rate for differet fission products of Np.-237 sample of 1.011 g weight for proton beam of 0.66 GeV energy located on section 4 of the QUINTA target.
- .

3. Measurement .
3.2 Results -cont.

- Moreover, considering the two different actinide neptunium 237 samples after irradiation we have focused on the neutron capture (n,γ) reaction leading to formation of Np-238. From gamma-ray spectrum of the irradiated Np-237 we have selected five gamma ray lines shown in Table 3, which we have used to evaluate the capture rate per one gram of Np-237 and per one deuteron applying the equation presented above.

Table 3. Gamma line data of Np.-238 formed in Np-237(n,γ)Np-238 reaction.

Isotope	$T_{1/2}$	γ Line [keV]	I_γ [%]
Np-238	2.117d	984.45 1028.54 1025.87 923.98	27.8 20.38 9.65 2.869

- Neutron capture (n,γ) reaction was used for transmutation and γ-rays of the product nuclei was measured:
- $^{237}Np(n,\gamma)\ ^{238}Np$ (β^- , $T_{1/2}$ = 2.12 d) ⇒ short lived decay chain.

3. Measurement .
3.2 Results -cont.

Fig. 4

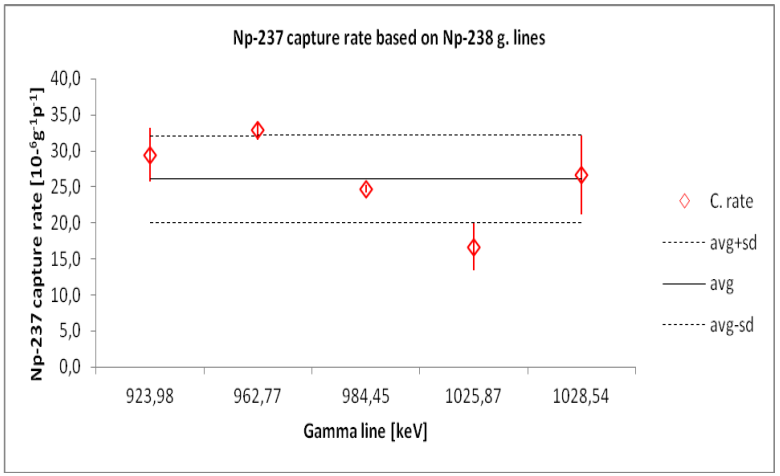

Fig. 4a

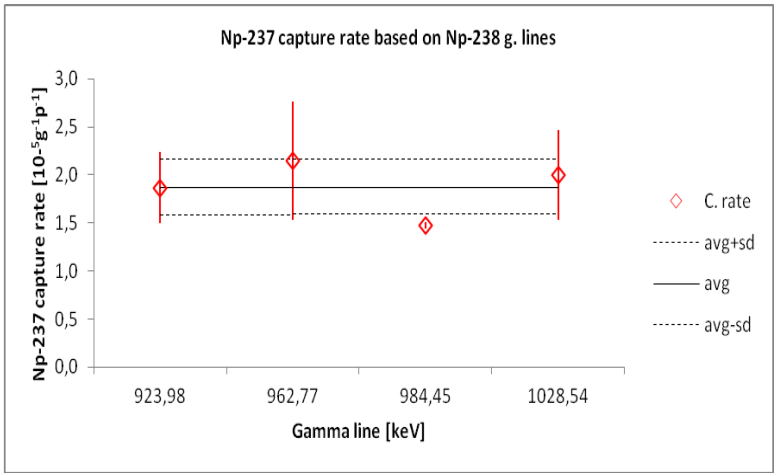

- The resulting normalized capture rate values are presented in Fig. 4 and Fig.4a for proton beam of 0.66 GeV and for the samples located on section 2 and 4 respectively:
- Fig. 4. Capture rate for different gamma lines of Np-238 for proton beam of 0.66 GeV energy for Np.-237 sample of 0.987 g weight located on section 2 of the QUINTA target.
- Fig. 4a. Capture rate for different gamma lines of Np-238 for proton beam of 0.66 GeV energy for Np.-237 sample of 1.011 g weight located on section 4 of the QUINTA target.

3. Measurement .
3.2 Results -cont.

Table 4. Compilation of incineration rate and capture rate of Np.-237 results.

Proton beam energy	**Ed = 0.66 GeV**	
Proton fluency	**$7.78\ 10^{14}$**	
Mass of Np.-237 sample [g]	0.987	1.115
Fission rate per gram sample and proton	$(2.82\ 10^{-5} \pm 0.418) \times 10^{-5}$	$(1.26 \pm 0.319) \times 10^{-5}$
Capture rate per gram sample and proton.	$(2.61 \pm 0.607) \times 10^{-5}$	$(1.87 \pm 0.290 \times 10^{-5}$
Fission/Capture rate	1.08±0.3	0.67±0.20

Applying the try and error method we find the neutron energy for which the ratio of fission cross section to capture cross section of the actinide Np-237 from the nuclear data base is equal to the measured ratio of fissioned and captured actinide isotopes (see next slide).

3. Measurement .
3.2 Results -cont.

Table 5. The fission/absorption ratios in function of neutron energy for neptunium 237

Neutron energy [MeV]	Fission cross section σ(n,f) [barn]	Capture cross section σ(n,γ) [barn]	σ(n,f)/ σ(n,γ)
0.448	0.319	0.564	0.299
0.449	0.322	0.479	0.672
0.450	0.325	0.477	0.681
0.492	0.456	0.426	1.070
0.493	0.458	0.423	1.082
0.494	0.460	0.422	1.090

- In Table 5 are collected several fission and capture cross sections and neutron energies extracted from data base ENDF/B-VII.1 for the distinct neutron energy.
- The red colors show the neutron energies for which the ratios of fission to capture are equal to the measured ratios.
- It means that the retrieved distinct fission and capture cross sections for the distinct neutron energy describe the average values.

3. Measurement .
3.2 Results -cont.

Table 6. Neutron fluencies measured for two samples located on section 2 and section 4 of the QUINTA target irradiated with proton beam of 0.66 GeV energy.

Sections of the QUINTA target	**2**	**4**
Neutron fluence using for evaluation the number of fissions in the sample [n/cm^2] x10^{13}	1.88	1.197
Neutron fluence using for evaluation the number of captures in the sample [n/cm^2] x10^{13}	1.89	1.189
Average neutron energy [MeV]	0.493	0.449

- The obtained values for average fission and capture cross sections in Table 5. let us to evaluate the neutron fluencies by help of the equations (Eq. 1. and Eq. 2.)
- In Table 6. are collected the neutron fluencies evaluated for two samples located on section 2 and section 4 of the QUINTA.

3. Measurement .
3.2 Results -cont.

- As it was expected the neutron fluencies evaluated using the measured number of fissions in the sample and the measured number of captures in the sample gave (nearly) the same values (see Table 6) within the error accuracy (within the standard deviation) in both experiments what is a proof for correct measurements. The precision of this method is estimated to be around 25 %?
- Adding the values of neutron fluencies measured by the silicon detector method we can compare the two methods. This is collected in Table 7.

3. Measurement .
3.2 Results -cont.

Table 7. Compilation of neutron fluencies measured by two methods for the two experiments

Sections of the QUINTA target	2	4
Neutron fluence using for evaluation the number of fissions in the sample [n/cm^2] x10^{13}	1.88	1.197
Neutron fluence using for evaluation the number of captures in the sample [n/cm^2] x10^{13}	1.89	1.189
Average neutron energy [MeV]	0.493	0.449
Neutron fluence using silicon detectors [n/cm^2] x10^{13}	**1.59**	**0.686**

3. Measurement .
3.2 Results -cont.

- From Table 7 we see that:
- - The difference between measured fluencies by the considered two methods for samples placed on the second section of the QUINTA target is 0.29 10^{13}, which is about 15% of the measured values, where the average neutron energy was 0.493.
- - However, the difference between measured fluencies by the considered two methods for samples placed on the forth section of the QUINTA target is 5.11 10^{12}, which is about 42% of the measured values, where the average neutron energy was 0.449.
- - The difference between the average energies of neutrons of these two positions (locations, places) is 0.044 MeV.

4. Discussion

- Neutron damage in the silicon detector placed in certain neutron spectrum collects the damage from whole spectrum starting from neutron energy as a threshold equal to 170 KeV to very high energy about 50 MeV irrespectively of its energy (see Fig. 2 – red line). It is an additive process. So the reverse dark current in the silicon detector is proportional to the average damage done by the neutrons of actually existing neutron spectrum in this range.

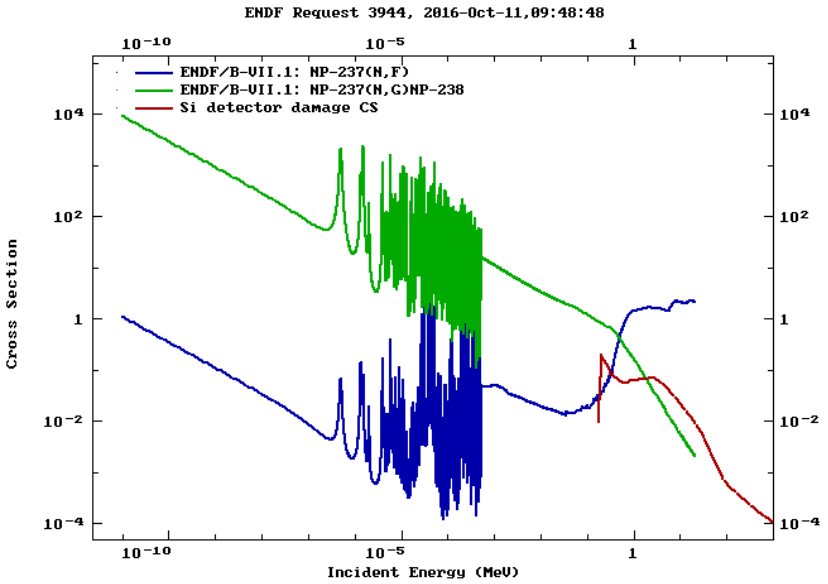

Fig. 2. Cross section of neutron inducing damage in the silicon detector (red curve [4]) and cross sections of neutron inducing fission and capture on Np-237 minor actinide.

4. Discussion.

- In the earlier experiment, presented in the paper [1], when the average neutron energy was equal to 0.452 MeV and the difference of neutron fluency measurement between the two methods was about 35 % .
- In the current experiment when the average neutron energy is equal to 0.449 MeV, the difference of neutron fluency measurement between the two methods is about 42 %. While for the average neutron energy equal to 0.493 MeV, the difference of neutron fluency measurement between the two methods is about 15 %.
- We can see certain regularity in the measurements, the higher is the average neutron energy the smaller is the difference of neutron fluency measurement between the two methods [see Table 8 – see in the next slide]. This effect was expected since the silicon detector method effectively measure the fast neutrons of energy higher than 170 keV.

4. Discussion.

Table 8. Compilation of neutron fluencies measured by two methods for three experiments in terms of average neutron energy.

Average neutron energy [MeV]	0.493	0.452	0.449
Neutron fluence using for evaluation the number of fissions in the sample [n/cm^2] x10^{13}	1.88	1.67	1.197
Neutron fluence using for evaluation the number of captures in the sample [n/cm^2] x10^{13}	1.89	1.64	1.189
Neutron fluence using silicon detectors [n/cm^2] x10^{13}	**1.59**	**1.11**	**0.686**
Difference of neutron fluency measurement between the two methods [%]	15	35	42

The difference of two fast neutron fluence measurements gives estimation of neutron fluence for the neutron energy below 170 keV - the additional approach.

4. Discussion.

- It is widely known that the average neutron energy during the process of fission is about 2 MeV but during the process of spallation is about 3 MeV.
- The quotient of cross sections for fission and capture for these neutron energies (2 an 3 MeV) gives information on incineration of minor actinides. This is clearly seen in Table 9 (see next slide) where are collected the mentioned parameters for these neutron energies extracted from the data base ENDF/B-VII.1.

4. Discussion.

Table 9. The fission/absorption ratios in function of neutron energy for neptunium 237 and americium 241.

Neutron energy [MeV]	Fission cross section σ(n,f) [barn]	Capture cross section σ(n,γ) [barn]	σ(n,f)/ σ(n,γ)
Np-237			
1.0	1.4587	0.17277	8.43213
2.0	1.7001	0.06090	27.9664
3.0	1.6609	0.032674	50.8339
Am-241			
1.0	1.2615	0.292707	4.30977
2.0	1.8498	0.07717	23.9701
3.0	1.85973	0.02145	86.6827

4. Discussion

- The minor-actinide-bearing blanket (MABB) concept [5, 6] is based on irradiation of such blankets containing a significant quantity of minor actinides in a solid solution mixed with uranium oxide which is to be located in radial blankets on the periphery of the outer core in a sodium-cooled fast reactor (SFR).

- Inside in the structure of fuel the average neutron flux can be very close to the average energy of fission neutrons what ensure that the incineration efficiency is within the range of 8 – 27 times higher for Np-237 and 4 - 23 times higher for Am-241 than production of next actinides (see Table 9 – previous slide).

4. Discussion

- This analytical and experimental analysis suggests that ADS can be even more efficient in incineration of minor actinides because the spallation source can be build from the minor actinides in a solid solution mixed with uranium oxide and located in the center of the ADS core where neutron flux is higher than in the periphery of the SFR core and its neutron flux is more hard what ensure that the incineration efficiency is within the range of 27 – 50 times higher for Np-237 and 23 - 86 times higher for Am-241 than production of next actinide (see Table 9).
- The behavior under irradiation of such spallation source and its close surrounding constituting the reactor core containing a significant quantity of minor actinides in a solid solution mixed with uranium oxide must nevertheless be studied and characterized in greater detail.

5. Conclusions

- Minor actinide samples and planar silicon detectors can be used as neutron fluence detectors especially in the high neutron energy range that is difficult to measure.
- Given the importance of high energy neutron measurement in the ADS (Aclerator Driven System) the actinide and silicon detectors could be a very useful tool for research of the minor actinides incineration efficiency.
- The difference of two fast neutron fluence measurements of the two presented above methods gives additionally estimation of neutron fluence for the neutron energy below 170 keV – the additional approach.
- The higher is the average neutron energy the smaller is the difference of neutron fluency measurement between the two methods.

6. References.

- [1] M. Szuta, S. Kilim, E. Strugalska-Gola, M. Bielewicz, N.I. Zamyatin, A. I Shafronovskaya, S. Tyutyunnikov; Comparison of two fast neutron fluence measurement methods based on Np237 fission to capture ratio measurement (spectral index) and a reverse dark current measurement of planar silicon detector; XXIII International Baldin Seminar on High Energy Physics Problems – "Relativistic Nuclear Physics & Quantum Chromodynamics"; Russia, Dubna, September, 2016.; *Baldin ISHEPP XXIII;* EPJ Web of Conferences **138** 10006 (2017), DOI: 10.1051/epjconf/201713810006
- [2] N. I. Zamyatin, A. E. Cheremukhin, and A. I. Shafronovskaya; Measuring Fluence of Fast Neutrons with Planar Silicon Detectors; Physics of Particles and Nuclei Letters, 2017, Vol. 14, No. 5, pp. 762–777.
- [3] I.A. Golutvin et al., "Radiation hardness of silicon detectors for collider experiments", preprint E14-95-97, Dubna 1995.
- [4] Van Ginneken A. Non ionizing energy deposition in silicon for radiation damage studies: Fermi Nat. Accelerator Lab. Report FN-522.-1989

6. References.

- [5] B. Valentin, H. Palancher, C. Yver, V. Garat, S. Massara, “Heterogeneous Minor Actinide Transmutation on a UO2 blanket and on (U,Pu)O2 fuel in a SFR – Preliminary design of pin and assembly”, Proc. Int. Conf. GLOBAL 2009, Paris, France, Sept. 6-11, 2009.
- [6] Syriac BEJAOUI, Elio D’AGATA, Ralph HANIA, Thierry LAMBERT, Stéphane BENDOTTI, Cédric NEYROUD, Nathalie HERLET, Jean-Marc BONNEROT ; Americium-Bearing Blanket Separate-effect Experiments:MARIOS and DIAMINO Irradiations; Proceedings of GLOBAL 2011 Makuhari, Japan, Dec. 11-16, 2011 Paper No. 503621

- Thank you for the attention.